

A study of thermal vorticity in PICR hydrodynamic model

Yilong Xie¹, Gang Chen¹, and Laszlo Pal Csernai^{2,3}

¹ School of Mathematics and Physics, China University of Geosciences (Wuhan), Lumo Road 388, 430074 Wuhan, China

² Department of Physics and Technology, University of Bergen, Allegaten 55, 5007 Bergen, Norway

³ Frankfurt Institute for Advanced Studies, Ruth-Moufang-Strasse 1, 60438 Frankfurt am Main, Germany

Received: date / Revised version: date

Abstract. With a Yang-Mills field, stratified shear flow initial state and a high resolution (3+1)D Particle-in-Cell Relativistic (PICR) hydrodynamic model, we calculate thermal vorticity for peripheral Au+Au collisions at different energies $\sqrt{s} = 7.7 - 200$ GeV. Based on the thermal vorticity calculations, we investigate the two puzzles in Λ polarization studies: the global polarization splitting between Λ and $\bar{\Lambda}$, and local polarization/vorticity structure along the beam direction. Based on the vector meson field mechanism, we calculate the polarization splitting between Λ and $\bar{\Lambda}$, the results fit to the experimental results fairly well. We also confirm that thermal vorticity along the beam direction has a quadrupolar structure on transverse space plane $[x, y]$. Interestingly the quadrupolar structure takes time to form and will significantly weaken at later times. Besides, we find that the magnitude of z -directed thermal vorticity actually increases with the collision energy.

PACS. 25.75. -q – 25.75. Ld – 47.50. Cd

1 Introduction

Non-central heavy ion collisions create a participant system of extremely hot and dense matter, carrying substantial angular momentum that is perpendicular to the reaction plane [1, 2, 3]. Through the spin-orbital coupling, just as the Einstein-de-Hass effect [4] and Barnett effect [5] had revealed, the initial fireball angular momentum will eventually give rise to the spin alignment of final particles, such as Λ hyperons [6, 7]. The Λ hyperon reveals its polarization by emitting preferentially the weak decay products along its spin direction, and thus is a fairly good choice of polarization measurement in experiments [8, 9, 10]. Many theories and simulations were also addressing this topic [6, 11, 12, 13].

Recently, the STAR collaboration measured the non-vanishing Λ polarization for Au-Au collisions at different energies $\sqrt{s_{NN}} = 7.7$ GeV - 200 GeV [14, 15, 16], and as far as we know, the results conform with the theoretical predictions and simulations in two significant aspects: the global polarization of both Λ and $\bar{\Lambda}$ aligns with the initial angular momentum, and decreases with the energy; the local polarization along the beam direction shows quadrupolar structure on transverse momentum plane.

However, there still exist some puzzles in this field [17]. Globally, the magnitude of $\bar{\Lambda}$ polarization is larger than that of Λ polarization. Some might argue that due to the large errors in measurements, it is not sure that whether this polarization splitting really exists, but at least for collision energy of $\sqrt{s} = 7.7$ GeV, this splitting clearly exists

and the difference could be 3% at least (see Fig. 1). This splitting effect has raised large interests. It was proposed that the magnetic field induced by the charged spectators can give rise to the polarization splitting between Λ and $\bar{\Lambda}$, but this will require a magnetic field that is long lasting and has a large magnitude. These are not realized. A recent suggestion is that the magnetic field can also be induced by charged particles in vortical Quark-Gluon-Plasma (QGP), and in this scenario the magnetic field could last long enough until freeze-out, but problem still exists: the charge density might not be large enough to produce a magnetic field that is strong enough. E.g., the upper limits of the estimated polarization difference at 7.7 GeV is below 1%, which is far away from the lower boundary of experimentally observed 3% [18] difference.

Another novel mechanism was proposed by Ref. [19], that the vector meson's strong interaction "magnetic" field, induced by the baryon vorticity at freeze-out, can split the polarization. However, the polarization splitting formula therein is driven mainly by the directed flow coefficient (c_1) and the shear flow coefficient (c_3) [19]. The coefficient C , which is proportional to $\Delta c = c_1 - c_3$, is actually a free parameter. Therefore, in this paper, we are going to revisit the theory in Ref. [19] and modify the splitting formula therein, (mainly by removing the free parameter C). Then based on this vector meson field mechanism, we use the high resolution (3+1)D Particle-in-Cell Relativistic (PICR) hydrodynamic model, used in several earlier estimates, to simulate and calculate the polarization splitting effect.

Locally, the longitudinal polarization on transverse momentum plane, from model simulations of both a multiple phase transport (AMPT) model [20] and the hydrodynamic simulations [21], exhibits opposite signature to the experimentally observed quadrupolar structure. However, our recent work [22] using the PICR hydrodynamic model to calculate the polarization at 200 GeV Au-Au, shows a fairly good agreement to the experimentally observed longitudinal polarization, in two aspects: 1) the sign distribution is (+, -, +, -) counting from the first quadrant to fourth quadrant of transverse momentum coordinate, 2) the peak value at transverse momentum $p_t = 1.4$ GeV has similar magnitude with the global polarization.

Besides, some interesting points emerge: the longitudinal polarization in our model was found to increase with collision energy, which differs with the energy dependence of the global polarization and contradicts a previous prediction [21] that the z-directed polarization tends to decrease with collision energy. In our model the first term in the polarization vector formula arising from the classic thermal vorticity, still has a sign structure of (-, +, -, +), but will be suppressed by the second term's opposite signature and resulting in a smaller but correct magnitude. Thus, in this paper, we are going to explore the classic thermal vorticity in the beam direction, showing its spatial structure, time evolution and magnitude changing tendency, etc.

Therefore, in this paper we want to explore the above two puzzles in the A polarization studies. The paper is organized as follows. Firstly, we revisit the theory in Ref. [19], and then use the PICR hydrodynamic model to simulate and calculate the polarization splitting at different energies $\sqrt{s_{NN}} = 7.7 - 200$ GeV. The averaged thermal vorticity along the $-y$ direction at freeze out as a function of energy are also shown. Secondly, subsequent to our previous work [22], we study the classic thermal vorticity along the beam direction. Finally, a summary is drawn. Throughout this paper, we use the natural units: $\hbar = c = k_B = 1$.

2 Polarization splitting induced by baryonic vorticity

2.1 Revisiting the theory

Considering the strong interaction of any fermions mediated by any bosonic fields, one could always write down a general equation of Lagrangian density

$$\mathcal{L} = \mathcal{L}_f + \mathcal{L}_b + \mathcal{L}_{int}. \quad (1)$$

where \mathcal{L}_f denotes the Lagrangian density for the fermions, \mathcal{L}_b represents the Lagrangian density for the bosons, and \mathcal{L}_{int} is the interaction Lagrangian density between them. In a simplest case, this equation can be written as:

$$\begin{aligned} \mathcal{L} = & \sum_i \bar{\psi}_i (i \not{\partial} - m_i + f_\sigma g_\sigma \sigma - f_V g_V \not{V}) \psi_i \\ & + \frac{1}{2} (\partial_\mu \sigma \partial^\mu \sigma - m_\sigma^2 \sigma^2) - \frac{1}{4} V^{\mu\nu} V_{\mu\nu} + \frac{1}{2} m_V^2 V_\mu V^\mu, \quad (2) \end{aligned}$$

where the first line corresponds to $(\mathcal{L}_f + \mathcal{L}_{int})$, denoting the Lagrangian density of Dirac field for fermions with a Yuwaka interaction coupling. The second line corresponds to \mathcal{L}_b , being the Lagrangian density for the scalar boson σ and vector boson V_μ . Here, g_σ is the coupling constant between fermion ψ_i (of species i) and the scalar boson σ , and g_V is the coupling constant between the fermion ψ_i and the vector boson V_μ . m_i , m_σ and m_V are respectively the mass of baryon, scalar meson and vector meson. The vector meson tensor is: $V_{\mu\nu} = \partial_\mu V_\nu - \partial_\nu V_\mu$. The two constants, f_σ and f_V in the Yuwaka interaction term are parameters that should be determined case by case.

In relativistic heavy ion collisions, the hyperons are created at the chemical freeze out and then interact with other particles during the hadronic scattering phase. Given that the strong interaction of baryons (including hyperons) with other particles is mediated by a scalar meson field σ and a vector meson field V^μ , then with the constants $f_\sigma = f_V = 1$, and following from the Euler-Lagrange equations, one finds the equations of motion for these fields:

$$[\gamma^\mu (i \partial_\mu - g_{Vi} V_\mu) - (m_i - g_{\sigma i} \sigma)] \psi = 0, \quad (3)$$

$$\partial_\mu \partial^\mu \sigma + m_\sigma^2 \sigma = \sum_i g_{\sigma i} n_{si}, \quad (4)$$

$$\partial_\mu V^{\mu\nu} + m_V^2 V^\nu = \sum_i g_{Vi} J_i^\nu, \quad (5)$$

where $n_{si} = \langle \bar{\psi} \psi \rangle$ is the scalar density of species i , and $J_i^\mu = \langle \bar{\psi} \gamma^\mu \psi \rangle$ is the baryon current of species i . These equations are actually the Dirac field equations with scalar and vector field coupling, the Klein-Gordon equation and the Proca equations. The detailed treatments of the above three equations has been demonstrated in Ref. [19]. In this subsection we will simply revisit the theory and modify it in a way that is suitable to our simulations.

For the Proca equation (5), analogous to Maxwell equations of massless photon field, it could be decomposed into Maxwell-Proca equations for vector mesons

$$\nabla \cdot \mathbf{E}_V = \bar{g}_V \rho - m_\sigma^2 V_0, \quad \nabla \cdot \mathbf{B}_V = 0 \quad (6)$$

$$\nabla \times \mathbf{E}_V + \frac{\partial \mathbf{B}_V}{\partial t} = 0, \quad \nabla \times \mathbf{B}_V - \frac{\partial \mathbf{E}_V}{\partial t} = \bar{g}_V \mathbf{J}_B + m_V \mathbf{V}, \quad (7)$$

where \bar{g}_V is the mean coupling constant of vector meson, the baryon density is $\rho_B = \sum_i \psi_i^\dagger \psi_i$ and the baryon (three-)current is \mathbf{J}_B . These are components of the baryon (four-) current $J_B^\nu = (\rho_B, \mathbf{J}_B) = \sum_i \bar{\psi} \gamma^\nu \psi$. Here the \mathbf{E}_V & \mathbf{B}_V are the 'electric' and 'magnetic' components of the vector meson field, defined as:

$$E_i \equiv V_{i0} = \partial_i V_0 - \partial_0 V_i = (-\nabla V_0 - \frac{\partial \mathbf{V}}{\partial t})_i, \quad (8)$$

$$B_i \equiv -\frac{1}{2} \epsilon_{ijk} V^{jk} = -\frac{1}{2} \epsilon_{ijk} (\partial^j V^k - \partial^k V^j) = (\nabla \times \mathbf{V})_i, \quad (9)$$

where $i, j, k = 1, 2, 3$. Let us take the curl of Maxwell-Proca equations (7), and we obtain

$$\frac{\partial^2 \mathbf{E}_V}{\partial t^2} - \nabla^2 \mathbf{E}_V + m_V^2 \mathbf{E}_V = -\bar{g}_V (\nabla \rho_B + \frac{\partial \mathbf{J}_B}{\partial t}), \quad (10)$$

$$\frac{\partial^2 \mathbf{B}_V}{\partial t^2} - \nabla^2 \mathbf{B}_V + m_V^2 \mathbf{B}_V = \bar{g}_V (\nabla \times \mathbf{J}_B). \quad (11)$$

An analytic solution is possible, e.g. for magnetic fields:

$$\mathbf{B}_V(x) = \int dy \bar{g}_V (\nabla \times \mathbf{J}(y)) \int \frac{d^4 p}{(2\pi)^4} \frac{e^{-ip(x-y)}}{-p^2 + m^2} \quad (12)$$

where x, y are the space-time points, and p, m are the four-momentum and mass of the vector meson V^μ . However, a simple solution was obtained:

$$\mathbf{B}_V = \frac{\bar{g}_V}{m_V^2} (\nabla \times \mathbf{J}_B). \quad (13)$$

by neglecting the derivatives in eqs. (10, 11) due to large meson mass, $m_\omega = 783$ MeV and $m_\sigma = 550$ MeV. Assuming local equilibrium of the system during the hadron scattering, i.e. the small gradients, $\nabla \rho \approx 0$, then for the current $\mathbf{J}_B = \rho_B(\mathbf{x}, t) \mathbf{v}(\mathbf{x}, t)$,

$$\nabla \times \mathbf{J}_B = \rho_B (\nabla \times \mathbf{v}) = \rho_B \boldsymbol{\omega}, \quad (14)$$

where $\boldsymbol{\omega}$ is the vorticity of baryon current. Therefore, we could see that the vortical baryon current will induce a vector meson's 'magnetic' field, which, together with the vector meson's 'electric' field, follow from the Maxwell-Proca equations (6,7) and definition equations (8,9).

Then the Zeeman energy term in the Foldy-Wouthuysen (FW) Hamiltonian for the hyperon particle's spin (with effective mass M_H) and the vector meson's magnetic fields was written as [19]:

$$H_{\text{spin-B}}^V = -\frac{g_{VH}}{M_H} \beta \mathbf{S} \cdot \mathbf{B}_V. \quad (15)$$

where it was argued that the constant matrix β will result in the opposite signs for Λ and $\bar{\Lambda}$, thus it may be responsible for the polarization splitting.

Supposing that spin-1/2 hyperons are at local equilibrium, one could add into the density matrix of the system, ρ , an extra term $\rho_s \sim \exp(\hat{\mathbf{S}} \cdot \boldsymbol{\Omega}/T)$, where $\boldsymbol{\Omega} = \mu \mathbf{B}_V/S = 2\mu \mathbf{B}_V$ is the vector meson's 'magnetic moment' with $\mu = -(g_{VH}/M_H)\beta$ being the 'magneton'. The ensemble average of the spin vector of spin-1/2 particles are given as $\mathbf{S} = \text{tr}(\rho \hat{\mathbf{S}})$ where $\hat{\mathbf{S}}$ is the spin operator. Then the ensemble averaged polarization vector can be obtained as [23]

$$\mathbf{P} = 2\mathbf{S} = \tanh\left(\frac{\boldsymbol{\Omega}}{2T}\right) \hat{\boldsymbol{\Omega}} \simeq \frac{\boldsymbol{\Omega}}{2T} = -\beta \frac{g_{VH}}{M_H} \frac{\mathbf{B}_V}{T}, \quad (16)$$

where $\hat{\boldsymbol{\Omega}}$ is the unit vector along $\boldsymbol{\Omega}$ direction. Taking eqs. (13) and (14) into the above equation, the polarization splitting would be

$$\Delta \mathbf{P} = \mathbf{P}_{\bar{H}} - \mathbf{P}_H = 2 \frac{g_{VH} \bar{g}_V}{M_H m_V^2} \frac{\rho_B \boldsymbol{\omega}}{T}. \quad (17)$$

Hence, if the baryons in high energy nuclear collisions have a vortical flow motion, the scalar and vector meson interactions given above can provide a mechanism for hyperon polarization splitting.

2.2 Polarization splitting at $\sqrt{s_{NN}} = 7.7 - 200$ GeV

The nucleus-nucleus impact in our initial state is divided into many slab-slab collisions, and Yang-Mills flux-tubes. These are assumed to form streaks [24,25]. In this scenario, the initial state naturally generates longitudinal velocity shear flow, which when placed into the subsequent high resolution (3+1)D Particle-in-Cell Relativistic (PICR) hydrodynamic model, will develop into substantial vorticity. Since our initial state+hydrodynamic model describes the shear and vorticity in heavy ion collisions fairly well, its simulations to the Λ polarization was also successful.

Therefore, we use the PICR hydrodynamic model to simulate the Au+Au collisions at RHIC BES energy region $\sqrt{s_{NN}} = 7.7 - 200$ GeV, and calculate the polarization difference between the $\bar{\Lambda}$ s and Λ s, based on eq. (17). The coefficients in eq. (17) are kept the same as in Ref. [19]: $M_\Lambda = 1115.6$ MeV, $M_V = 780$ MeV, $\bar{g}_V = 5$, and $g_{V\Lambda} \approx 0.55 g_{VN} \approx 4.76$.

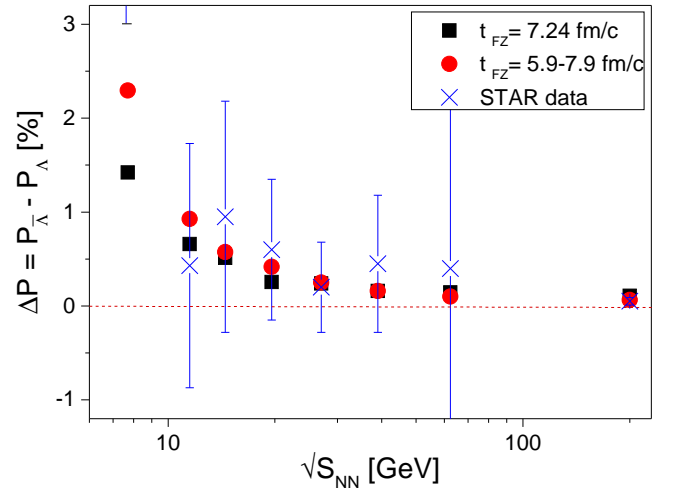


Fig. 1. (Color online) The polarization difference between Λ s and $\bar{\Lambda}$ s for Au+Au collisions at $\sqrt{s_{NN}} = 7.7 - 200$ GeV with impact parameter ratio $b_0 = 0.7$. The black squares represent the polarization difference as a function of collision energy, with the freeze-out time being fixed to $t_{FZ} = 7.24$ fm/c. The red circles correspond to the case of varied freeze-out time, i.e. $t = 5.9 - 7.9$ fm/c for the energy range of $\sqrt{s} = 7.7 - 200$ GeV. The experimental data denoted by cross symbols with error bars are extracted from Ref. [17].

For the purpose of continuity, we do not perform a new simulation, but just use the same data in our previous Rapid Communication [26], which was then the first

work to show the energy dependence of global polarization Π_{0y} , and exhibited fairly good agreement with the experimental data. In that work, the simulation parameters were set as follows: the impact parameter ratio is: $b_0 = b/b_{max} = 0.7$, (where b is the impact parameter and b_{max} is the maximum impact parameter); the cell size is 0.343^3 fm^3 , the time increment is 0.0423 fm/c ; the freeze-out time is chosen as $7.24 \text{ fm/c} = 2.5 + 4.74 \text{ fm/c}$ (2.5 fm/c for the initial state's stopping time and 4.74 fm/c corresponds to the hydro-evolution time).

The simulation and calculation results are shown in Fig. 1, which exhibits the polarization difference between Λ and $\bar{\Lambda}$ for Au+Au collisions at $\sqrt{s_{NN}} = 7.7 - 200 \text{ GeV}$. The black and red symbols respectively represent the polarization difference with freeze-out time t_{FZ} being fixed to $t_{FZ} = 7.24 \text{ fm/c}$, and with varied freeze-out time increasing from 5.9 to 7.9 fm/c (when collision energy increases from 7.7 to 200 GeV). The experimental data denoted by cross symbols with error bars are extracted from Ref. [17]. Obviously, our simulation results, by using the PICR hydrodynamic model, show good agreement with the STAR's experimental data.

For the case of 7.7 GeV, the difference from our model could be as significant as 2.3%, which is more than 2 times larger than the upper boundary estimate in Ref. [18]. However, our value of 2.3% is still smaller than the lower boundary of experimental measurement of 3%. Presently several mechanisms were proposed, and quantitative calculations were performed, to explain the Λ and $\bar{\Lambda}$ polarization splitting [19, 18, 27, 28], but none of them can achieve 3% difference at 7.7 GeV. If the experimental results are true, this might indicate the polarization splitting phenomenon is not induced by a single effect and needs a combined theory to explain.

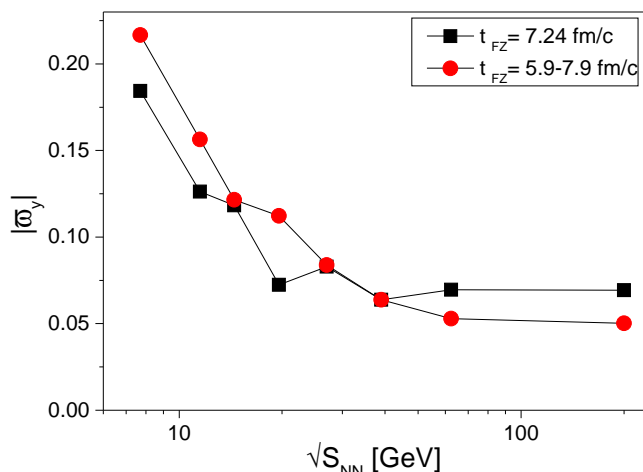


Fig. 2. (Color online) The y -directed thermal vorticity ϖ_y at freeze out as function of collision energy. The black and red symbols respectively represent the vorticity at fixed freeze-out time $t_{FZ} = 7.24 \text{ fm/c}$, and at varied freeze-out time $t_{FZ} = 5.9 - 7.9 \text{ fm/c}$.

Fig. 2 shows the thermal vorticity along the y direction, (averaged over the whole volume),

$$\langle \varpi_y \rangle = \langle [\nabla \times \frac{\hbar \mathbf{v}}{T}]_y \rangle, \quad (18)$$

as a function of collision energy (\hbar was absorbed into the calculation to have a dimensionless vorticity). It is not surprising that the y -directed thermal vorticity decreases with the collision energy, but the magnitude of the thermal vorticity in our model is larger than that from the AMPT simulation [29, 30].

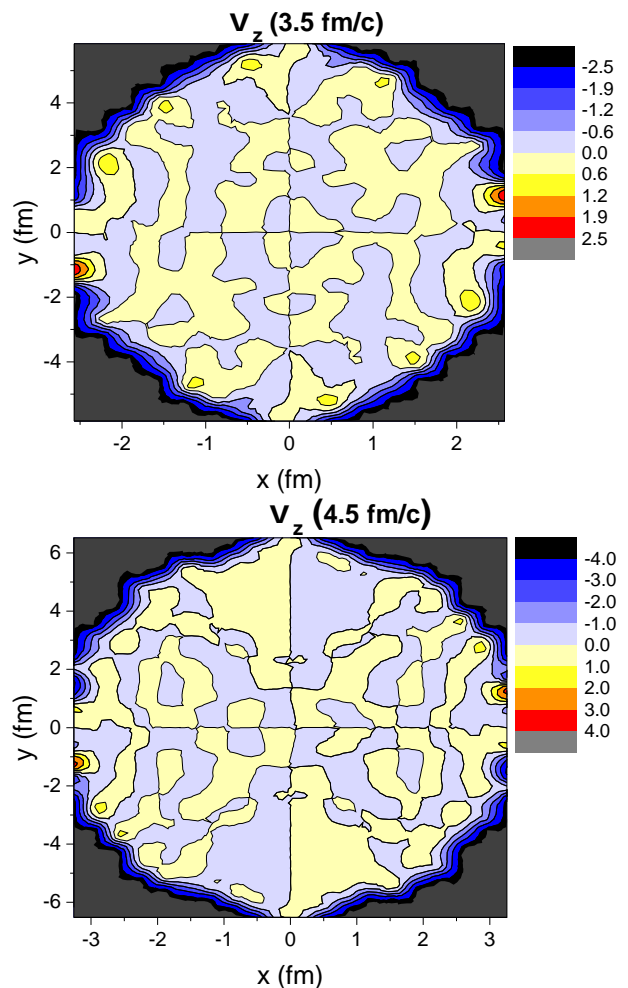


Fig. 3. (Color online) The averaged z -directed vorticity ϖ_y on transverse plane $[x, y]$, at different early evolution times, for Au+Au 200 GeV collisions.

Specifically, the thermal vorticity ϖ_y in our model for $\sqrt{s} = 39-200 \text{ GeV}$ is about 0.5 - 0.6, corresponding to the vorticity value of 0.15 - 0.25 in AMPT model.¹ Due to the large magnitude of vorticity created in our model, the

¹ The vorticity in Ref. [29] was defined as $\omega = \nabla \times \mathbf{v}$, which is not thermal vorticity defined herein. To compare, one could estimate the freeze-out temperature as around 170 MeV at $\sqrt{s} = 39 - 200 \text{ GeV}$ [31], and thus the factor $\frac{\hbar}{T} \approx 1.16 \text{ fm/c}$.

calculated splitting effect could be as significant as the experimental data, as demonstrated in Fig. 1.

3 Thermal vorticity along the beam direction

The longitudinal polarization as a function of azimuthal angle was observed to have a sine structure [17,32], as predicted by theory and simulations [33,21], that the longitudinal polarization at central rapidity shows a quadrupolar structure on transverse momentum plane.

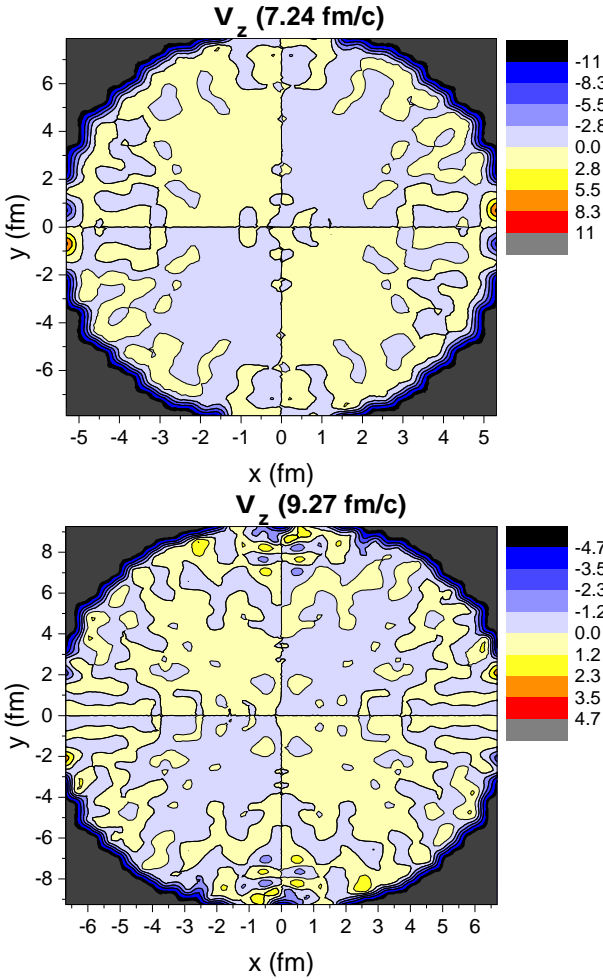


Fig. 4. (Color online) The averaged z -directed vorticity ϖ_y on transverse plane $[x, y]$, at different late evolution times, for Au+Au 200 GeV collisions.

Figs. 3 and 4 show the classic thermal vorticity along the beam direction,

$$\langle \varpi_z(x, y) \rangle = \langle [\nabla \times \frac{\hbar \mathbf{v}}{T}]_z \rangle, \quad (19)$$

on the transverse plane $[x, y]$, at different time $t = 3.5 - 9.27$ fm/c for Au+Au 200 GeV collisions. The average is performed over all z -layers, and weighted with local particle density n .

One could see that, it is until $t=7.24$ fm/c, i.e. the freeze-out time, that the ϖ_z shows a quadrupolar structure on the transverse space plane. Before freeze-out at $t = 3.5$ fm/c, the quadrupolar structure has not formed yet, and after freeze-out at $t = 9.27$ fm/c, the quadrupolar structure is significantly weakened, and tends to vanish. Another interesting point is that, it seems that the z -directed thermal vorticity's magnitude peaks around the freeze-out time, i.e. either pre- or post- freeze out, its magnitude is smaller. (We want to clarify that the freeze-out time in our model can be chosen freely, but in order to fit the global Λ polarization value measured at STAR 200GeV Au-Au collisions, the freeze-out time should be around $t=7.24$ fm/c).

Then we also extract the maximum value of ϖ_z on the transverse plane $[x, y]$ at freeze-out for different energies $\sqrt{s} = 11.5, 39, 200$ GeV, as shown in Fig. 5. This figure indicates that the thermal vorticity along the beam direction increases with collision energy, which differs from the energy dependence of y -directed vorticity as shown in Fig. 2. However, this is in line with our previous prediction that the longitudinal polarization's magnitude increases with collision energy [22]. If our results are true, the longitudinal polarization could be a non-trivial signal in higher energy collisions beyond RHIC energy region.

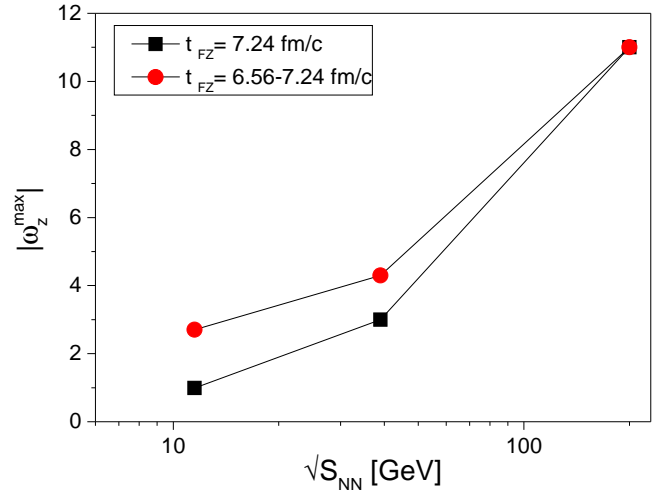


Fig. 5. (Color online) The extracted maximum z -directed thermal vorticity ϖ_z on transverse plane $[x, y]$, at freeze-out for different collision energies $\sqrt{s} = 11.5, 39, 200$ GeV. The black symbols correspond to fixed freeze-out time $t_{FZ} = 7.24$ fm/c, and the red ones correspond to varied freeze-out time $t_{FZ} = 6.56 - 7.24$ fm/c.

4 Summary and Conclusion

With the PICR hydrodynamic model, we study thermal vorticity along the y direction, ϖ_y , and along the beam direction, ϖ_z , as a function of collision energy. We found that the y -directed thermal vorticity, ϖ_y , is larger than the

one from the AMPT model, and when applied to calculate the polarization splitting between Λ and $\bar{\Lambda}$, the results fit to the experimental data fairly well. We also confirm that the z -directed thermal vorticity ϖ_z has a quadrupolar structure on transverse space plane, but interestingly the quadrupolar structure takes time to form and will be significantly weakened at late freeze-out. Besides, we find that the magnitude of z -directed thermal vorticity, ϖ_z , actually increases with the collision energy.

Acknowledgments

We thank Dujuan Wang for enlightened discussions. The work of L.P. Cs. is supported by the Research Council of Norway, and of Y. L. Xie is supported by the Fundamental Research Funds for the Central Universities (Grant No. G1323519234).

References

1. F. Becattini, F. Piccinini, and J. Rizzo, *Phys. Rev. C* **77**, 024906 (2008).
2. J.-H. Gao, S.-W. Chen, W.-T. Deng, and Z.-T. Liang, Q. Wang, and X.-N. Wang, *Phys. Rev. C* **77**, 044902 (2008).
3. V. Vovchenko, D. Anchishkin, L.P. Csernai, *Phys. Rev. C* **90**, 044907 (2014)
4. A. Einstein and W. de Haas, *Deutsche Physikalische Gesellschaft, Verhandlungen* **17**, 152 (1915).
5. S. J. Barnett, *Rev. Mod. Phys.* **7**, 129 (1935).
6. F. Becattini, V. Chandra, L. Del Zanna, and E. Grossi, *Annals of Phys.* **338**, 32 (2013).
7. F. Becattini, L.P. Csernai, D.J. Wang, *Phys. Rev. C* **88**, 034905 (2013).
8. I. Abt *et al.* (HERA-B Collaboration), *Phys. Lett. B* **638**, 415-421, (2006).
9. I. Selyuzhenkov *et al.* (STAR Collaboration), *J. Phys. G: Nucl. Part. Phys.* **32**, S557-S561 (2006).
10. B. I. Abelev *et al.*, *Phys. Rev. C* **76**, 024915 (2007).
11. Z.-T. Liang, and X.-N. Wang, *Phys. Rev. Lett.* **94**, 102301 (2005).
12. X.-G. Huang, P. Huovinen, and X.-N. Wang, *Phys. Rev. C* **84**, 054910 (2011).
13. B. Betz, M. Gyulassy, and G. Torrieri, *Phys. Rev. C* **76**, 044901 (2007).
14. B. I. Abelev *et al.* (STAR Collaboration), *Phys. Rev. C* **76**, 024915 (2007), [Erratum: *Phys. Rev. C* **95**, 039906 (2017)].
15. L. Adamczyk *et al.* (The STAR Collaboration), *Nature* **548**, 62 (2017).
16. J. Adam *et al.* (STAR Collaboration), *Phys. Rev. C* **98**, 014910 (2018).
17. T. Niida *et al.* (STAR Collaboration), Invited talk at Quark Matter 2018, May 13-19, 2018, Venice, Italy.
18. X. Y. Guo, J. F. Liao, E. K. Wang, arXiv:1904.04704.
19. L. P. Csernai, J. I. Kapusta, and T. Welle, *Phys. Rev. C* **99**, 021901(R) (2019).
20. Xiao-Liang Xia, Hui Li, Zebo Tang, and Qun Wang, *Phys. Rev. C* **98**, 024905 (2018).
21. F. Becattini and I. Karpenko, *Phys. Rev. Lett.* **120**, 012302 (2018).
22. Yilong Xie, Dujuan Wang, Laszlo P. Csernai, arXiv:1907.00773.
23. F. Becattini *et al.*, *Phys. Rev. C* **95**, 054902 (2017).
24. V. K. Magas, L. P. Csernai, and D. D. Strottman, *Phys. Rev. C* **64** 014901 (2001).
25. V. K. Magas, L. P. Csernai, and D. D. Strottman, *Nucl. Phys. A* **712** 167 (2002).
26. Y. L. Xie, D. J. Wang, L. P. Csernai, *Phys. Rev. C* **95**, 031901R (2017).
27. Z.-Z. Han, J. Xu, *Phys. Lett. B* **786**, 255 (2018).
28. O. Vitiuk, L. Bravina, E. Zabrodin, arXiv:1910.06292.
29. Y. Jiang, Z.-W. Lin, and J. F. Liao, *Phys. Rev. C* **94**, 044910 (2016).
30. D.-X. Wei, W.-T. Deng, and X.-G. Huang, *Phys. Rev. C* **99**, 014905 (2019).
31. F. Becattini, J. Manninen, M. Gazdzicki, *Phys. Rev. C* **73**, 044905 (2006)
32. J. Adam *et al.* (STAR Collaboration), *Phys. Rev. Lett.* **123**, 132301 (2019).
33. Y. L. Xie, M. Bleicher, H. Stöcker, D. J. Wang, and L. P. Csernai, *Phys. Rev. C* **94**, 054907 (2016).